Torsional Constraints on the Formation of Open Promoter Complexes on DNA Minicircles Carrying σ^{54}-Dependent Promoters†

Matloob Qureshi, Trevor Eydmann, Sara Austin, and Ray Dixon*

Nitrogen Fixation Laboratory, John Innes Centre, Colney Lane, Norwich, NR4 6SY, U.K.

Received January 21, 1997; Revised Manuscript Received July 18, 1997⊗

ABSTRACT: A topoisomer gel retardation assay has been used to examine the topological requirements for the formation of open promoter complexes on DNA minicircles carrying σ^{54}-dependent promoters. In the absence of intercalators, individual topoisomers carrying both the *nifL* and *nifF* promoters could be resolved as discrete species by electrophoresis, but exhibited anomalous electrophoretic behavior at relatively high negative superhelical density, indicative of a structural transition. In the presence of phosphorylated activator protein NTRC, ATP, and σ^{54} RNA polymerase holoenzyme, discrete topoisomer shifts were detected associated with the formation of open promoter complexes. At the *nifL* promoter open complexes could be formed on all negatively supercoiled topoisomers examined as well as on nicked circular DNA, but not on the $\Delta Lk = 0$ topoisomer or positively supercoiled DNA. Minicircles carrying the σ^{54}-dependent *glnA*p2 promoter could not be resolved in the electrophoresis system, but using a combination of potassium permanganate footprinting and topoisomerase I relaxation assays, we found in contrast to the *nifL* promoter, that open complexes were formed not only on negatively supercoiled topoisomers but also on relaxed minicircles and the $\Delta Lk = +1$ topoisomer. These results indicate there is a thermodynamic barrier to the formation of open complexes on DNA minicircles carrying the *nifL* promoter which is not evident at *glnA*p2.

Transcription initiation at σ^{54} (σ^{N})-dependent promoters is characterized by a number of mechanistic features that distinguish this promoter class from those recognised by sigma factors homologous to σ^{70}, the major vegetative sigma factor of *Escherichia coli* (Kustu et al., 1989; Merrick, 1993). While RNA polymerase holoenzyme containing σ^{54} ($E\sigma^{54}$) can recognize specific promoter sequences and, like $E\sigma^{70}$, form a closed complex with promoter DNA, the formation of open promoter complexes by this holoenzyme form is dependent on a specific class of activator protein which catalyzes this isomerization step in a reaction requiring the hydrolysis of a nucleoside triphosphate, commonly ATP or GTP. σ^{54}-dependent activators have some properties in common with eukaryotic enhancer binding proteins and can activate transcription at a distance, contacting downstream-bound $E\sigma^{54}$ via the formation of a DNA loop (Buck et al., 1987; Minchin et al., 1989; Reitzer et al., 1989; Wedel & Kustu, 1991; Su et al., 1990; Carmona & Magasanik, 1996) (Figure 1).

We have shown previously that transcription from the σ^{54}-dependent *Klebsiella pneumoniae nifL* promoter is extremely sensitive to changes in DNA supercoiling both *in vivo* and *in vitro* (Dixon et al., 1988). It has been proposed that this sensitivity may reflect a role for DNA supercoiling in modulating the aerobic/anaerobic response of the *nifL* promoter (Kranz & Haselkorn, 1986; Dimri & Das, 1988; Dixon et al., 1988) since superhelical density decreases upon the shift between anaerobic to aerobic growth conditions and *vice versa* (Dorman et al., 1988; Hseih et al., 1991). The

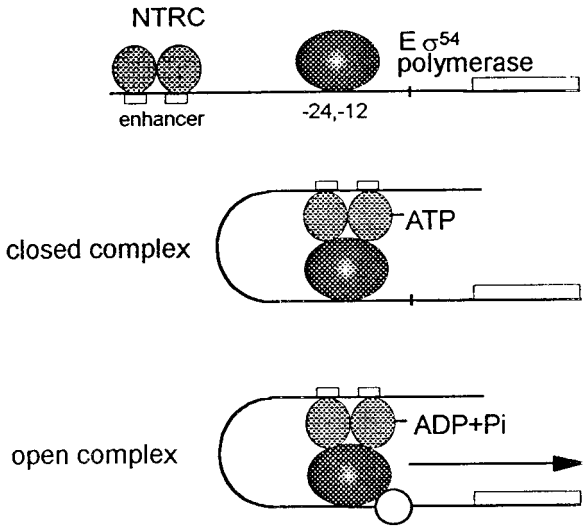

FIGURE 1: Schematic model for the formation of open complexes at σ^{54}-dependent promoters. Conserved promoter sequences for recognition by the σ^{54}-holoenzyme are located at −24 and −12 with respect to the transcription initiation site. Phosphorylated NTRC binds to upstream enhancer-like sequences comprising two dyad-symmetrical sites and contacts polymerase via formation of a DNA loop. NTRC catalyzes the isomerization of closed to open promoter complexes in a reaction that is dependent on the hydrolysis of ATP.

nifL promoter is activated at a distance by the nitrogen regulatory protein NTRC and at low activator concentrations, transcriptional activation is promoted by face-of-the-helix dependent interactions between upstream-bound NTRC and downstream-bound $E\sigma^{54}$ (Minchin et al., 1989). The supercoiling response of the promoter *in vitro,* as measured by the formation of open promoter complexes as a function of superhelical density, is biphasic and is influenced by at least three promoter elements. Mutations in either the $E\sigma^{54}$

† This research was supported by the Biotechnology and Biological Sciences Research Council. M.Q. was funded by a BBSRC postgraduate studentship.

* Corresponding author. Tel. +44 1603 456 900. FAX: +44 1603 454 970. E-mail: Ray.Dixon@bbsrc.ac.uk.

⊗ Abstract published in *Advance ACS Abstracts,* September 1, 1997.

recognition sequence or the region which is melted in open promoter complexes influence the response to superhelical density suggesting that both of these downstream promoter elements are functional in dictating the supercoiling response (Whitehall et al., 1992). Secondly, studies with hybrid promoters indicate that the upstream region of the *nifL* promoter which includes the activator binding sites also dictates the response to supercoiling, suggesting that supercoiling may stabilise DNA loop formation at this promoter (Whitehall et al., 1993). In contrast to *nifL*, the σ^{54}-dependent *glnA*p2 promoter, which is also activated by NTRC, is relatively insensitive to the level of DNA supercoiling *in vitro* (Ninfa et al., 1987; Dixon et al., 1988; Whitehall et al., 1992).

To gain more insight into the role of DNA supercoiling at σ^{54}-dependent promoters, we have utilized DNA minicircles to measure open complex formation on defined topoisomers. DNA minicircles have proved extremely useful for analyzing structural transitions in DNA (Nordheim & Meese, 1988; Gruskin & Rich, 1993) as well as DNA looping (Kramer et al., 1988), protein−DNA interactions (Bates & Maxwell, 1989; Douc-Rasy et al., 1989; Lavigne et al., 1994), and the binding of RNA polymerase (Kahn & Crothers, 1993; Su & McClure, 1994). We have determined the topoisomer preference for open complex formation at σ^{54} promoters on purified minicircles. At the *nifL* promoter open complexes form on negatively supercoiled topoisomers and nonconstrained molecules such as linear and nicked circular DNA. However their formation is not detected on relaxed minicircles or on the +1 topoisomer suggesting that these templates present a thermodynamic barrier to unwinding by Eσ^{54} at this promoter. In contrast, at the *glnA*p2 promoter, open complexes are formed not only on negatively supercoiled topoisomers but also on both the ΔLk = 0 and the +1 topoisomers demonstrating that the free energy requirements for open complex formation at the two promoters are different.

EXPERIMENTAL PROCEDURES

DNA Fragments. The 475 bp[1] *nifF*−*nifL* *Bam*HI fragment from pMS700L (Minchin et al., 1989) was cloned into the *Bam*HI site of pTE103 (Elliot & Geiduschek, 1984) to form pMAQ6. This plasmid was constructed to generate the FCL minicircle containing both the *nif*L and *nif*F promoters and the intergenic region (Figure 2). The fragment used to construct the FCL74 minicircle is identical with the exception of a G to T substitution at position −26 in the *nifL* promoter (Whitehall et al., 1992).

The 320 bp *Eco*RI−*Bam*HI fragment from pMS590 (Minchin et al., 1989), which lacks the *nif*F promoter, was ligated with a 37bp *Eco*RI−*Bam*HI double-stranded linker into the *Bam*HI site of pTE103 to generate pMAQ590. This plasmid carries a 357 bp *Bam*HI fragment used to generate the CL minicircle (Figure 2). Sequences of the linker oligo nucleotides were 5′-GATCCACTGACTGATGCATACCGTTAATTAATCGAGA-3′(top strand) and 3′-GTGACTGACTACGTATGGCAATTAATTAGCTCTTTAA-5′ (bottom strand).

The 305 bp *Eco*RI−*Bam*HI fragment from pTE595 (Minchin et al., 1989), which contains the downstream elements of the *nifL* promoter but lacks the specific NTRC binding sites, was ligated with a 33 bp double stranded

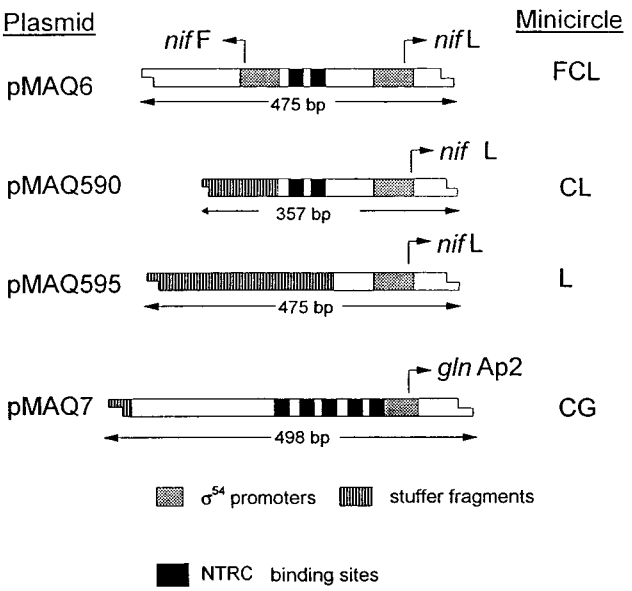

FIGURE 2: Diagrammatic representation (not to scale) of the DNA fragments used for minicircle construction. Further details are given in Experimental Procedures.

oligonucleotide with *Bam*HI and *Eco*RI compatible ends and inserted into the *Bam*HI site of pTE103. The sequence of the linker oligonucleotides was as follows: 5′-GATCCACTGACTCTAGACTGAGATCTAGCTCTA-3′ (top strand) and 3′-GTGACTGAGATCTGACTCTAGATCGAGATTTAA-5′. The resultant plasmid was digested with *Xba*I and *Bgl*II, at sites internal to the oligonucleotide, and ligated with a 146 nucleotide *Nhe*I−*Bam*HI fragment from pBR322 to construct plasmid pMAQ595 (Figure 2). This plasmid carries a 475 bp *Bam*HI fragment used to generate the L minicircle.

Plasmid pMAQ7 was constructed by ligating a 484 bp *Nco*I−*Bam*HI fragment from pRD567 carrying the *gln*A promoter (Dixon, 1984) with a 14 bp *Bam*HI−*Nco*I double-stranded linker, into the *Bam*HI site of pTE103. This generates a 498 bp *Bam*HI fragment used to construct the CG minicircle (Figure 2). Sequences of the linker oligonucleotides were as follows: 5′-GATCCGCTCCAGGC-3′ (top strand) and 3′-GCGAGGTCCGGTAC-5′ (bottom strand).

Minicircle Preparation. *Bam*HI-digested fragments were purified from agarose gels, dephosphorylated with calf-intestinal alkaline phosphatase and then end-labeled with [γ-^{32}P]ATP using T4 polynucleotide kinase. Unincorporated label was removed by Sephadex G-50 chromatography and the fragments were then ligated overnight at 4 °C in ligation buffer (50 mM Tris-HCl, pH 8.0, 6 mM $MgCl_2$, 20 mM DTT, 1 mM ATP) containing T4 DNA ligase (8.5 units) and varying concentrations of ethidium bromide (0.5−5 μM). Ligation mixtures were then treated with SDS (0.5%) EDTA (25 mM) plus protease K (0.5 g L^{-1}) for 15 min at 37 °C, extracted with phenol−chloroform, and then further purified by Sephadex G-50 chromatography. The circular nature of minicircles was confirmed by digesting samples in *Exo*III buffer (20 mM Tris-HCl, pH7.8, 100 mM KCl, 6 mM $MgCl_2$, 0.1 mM Na_2EDTA, 10 mM β-mercaptoethanol) with 10 units of exonuclease III for 30 min at 37 °C.

Topoisomer Identification and Purification. Topoisomer populations from ligations were run on 4% polyacrylamide gels (acrylamide:bisacrylamide ratio 80:1) in TBE buffer (45 mM Tris, 45 mM boric acid, 1 mM EDTA, pH 8.3) containing chloroquine (5−7.5 mg L^{-1}) in the gel and

[1] Abbreviations: bp, base pair(s); EDTA, ethylenediaminetetraacetic acid; DTT, dithiothreitol; SDS, sodium dodecyl sulfate.

running buffer. Topoisomers were identified by their consecutive appearance in ligations containing increasing concentrations of ethidium bromide. In the absence of intercalator, ligations produced a mixture of the $\Delta Lk = +1$ and relaxed topoisomers. Relaxed closed circular DNA was identified on the basis that it co-migrated with nicked circular DNA in the absence of chloroquine. Individual topoisomers were extracted from gel slices by electroelution, followed by phenol−chloroform extraction and ethanol precipitation.

Proteins. RNA polymerase core enzyme, σ^{54}, and NTRC were purified as described previously (Whitehall et al., 1992).

Open Complex Formation. Assays were performed in TAP buffer (50 mM Tris-acetate, pH 7.9, 100 mM potassium acetate, 8 mM magnesium acetate, 27 mM ammonium acetate, 1 mM DTT, 3.5% polyethylene glycol 6000) in the presence of 100 nM core RNA polymerase, 300 nM σ^{54}, varying concentrations of NTRC, 10 mM carbamoyl phosphate, 3.3 mM ATP, 3.4 mg mL^{-1} sonicated salmon sperm DNA, and 10−50 pM minicircle topoisomers in a total volume of 15−20 μL. Protein−DNA complexes were usually allowed to form for 20 min at 37 °C.

Gel Retardation Analysis. One-tenth volume of loading dye (0.1% xylene cyanol, 0.05% bromophenol blue, 50% glycerol) was added to preformed protein−DNA complexes which were immediately loaded onto a 4% (w/v) polyacrylamide gel (acrylamide:bisacrylamide ratio 80:1) in 25 mM Tris, 400 mM glycine, pH 8.6, which had been prerun at 180 V at room temperature down to a constant power of 2 W. Gels were run for around 4 h at 180 V (15 V per cm). After electrophoresis, gels were dried down and visualized by autoradiography. Radioactivity in complexes was quantitated with a Fujix BAS1000 phosphorimager.

Topoisomerase I Relaxation Assays. Preformed open complexes were treated with 10 units of wheat germ topoisomerase I (Promega) for 15 min at 37 °C. The reaction was stopped by the addition of SDS (final concentration 1%), and the mixture was allowed to stand on ice for 5 min before centrifugation at 12000*g* for 5 min at 4 °C. The supernatant was transferred to a new tube, extracted with phenol−chloroform, and following the addition of loading dye (one-tenth volume) was run on a 4% acrylamide TBE−chloroquine gel. Gels were visualised by autoradiography as described above.

DNA Ligase Assay for Protein-Dependent Unwinding. Preformed open complexes were treated with 8.5 units of T4 DNA ligase for 30 min at 37 °C. Reactions were stopped with SDS, processed, and run on chloroquine gels as described above for the topoisomerase assays.

$KMnO_4$ Footprinting. Open complexes formed on minicircle topoisomers were treated with $KMnO_4$ (8 mM) for 4 min at 37 °C before termination by the addition of 2 vol of stop mix (3 M ammonium acetate, 0.1 mM EDTA, 1.5 M β-mercaptoethanol, 100 mg/mL tRNA). Following extraction with phenol-chloroform and precipitation with ethanol, FCL minicircles were digested with *Bam*HI and *Alu*I, giving rise to 465 and 10 bp fragments. CG minicircles were digested with *Bam*HI and *Nco*I to give 484 and 14 bp fragments. The short fragments were too small to interfere with the analysis of the larger fragments on sequencing gels. For prelabeled minicircles this procedure allowed analysis of the bottom strand of the *nifL* and *glnA*p2 promoters. To analyze the top strand, complexes were formed on unlabeled minicircles which were subsequently 3′ end-labeled with [α^{32}P]dGTP after the *Bam*HI digestion. Following restriction enzyme digestion and end-labeling where necessary, the $KMnO_4$-treated DNA was cleaved with piperidine and the products were analyzed on 6% sequencing gels.

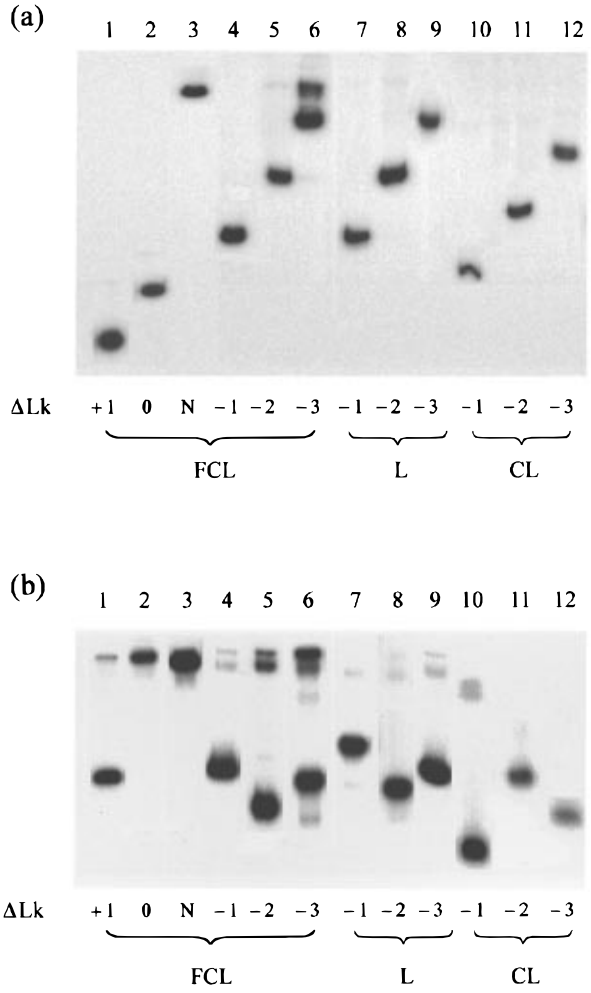

FIGURE 3: Electrophoretic mobilities of individual minicircle topoisomers after ligation of fragments in the presence of ethidium bromide and topoisomer purification. Linking number assignments and fragments circularized are indicated beneath each lane. (a) Electrophoresis was performed in TBE buffer in the presence of chloroquine (7.5 mg L^{-1}). (b) Electrophoresis was carried out in 25 mM Tris, 400 mM glycine, pH 8.6, as described for gel retardation analysis in Experimental Procedures.

RESULTS

We constructed a series of minicircles by ligation of end-labeled restriction fragments with T4 DNA ligase. The superhelical density of the products was varied by adjusting the ethidium bromide concentration in the ligation buffer. As expected, the ligation products were resistant to digestion by exonuclease III. The linking difference (ΔLk) of individual topoisomers was assigned on the basis of their mobilities on gels containing varying concentrations of chloroquine. In some cases the products contained a mixture of more than one topoisomer and were used directly although for most experiments individual topoisomers were purified by excision from the gel.

All of the minicircles are based on *BamH*I fragments and contain one or more σ^{54}-dependent promoters (Figure 2). The wild-type FCL minicircle contains the upstream region of the *nifL* promoter, including the tandem NTRC binding sites

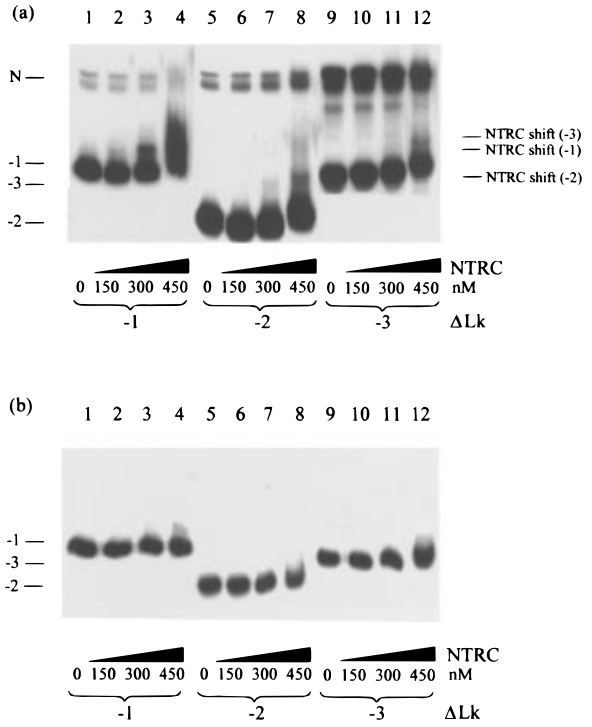

FIGURE 4: Binding of NTRC−phosphate to minicircle topoisomers. Purified topoisomers were incubated for 20 min at 37 °C with various concentrations of NTRC (indicated beneath each lane) in TAP buffer containing 10 mM carbamoyl phosphate, 3.3 mM ATP, and 3.4 mg L^{-1} sonicated salmon sperm DNA . Complexes were then run on Tris-glycine gels as described in Experimental Procedures. The mobility of free topoisomers is indicated on the left of each panel; N indicates nicked circular DNA. Protein−DNA complexes are indicated on the right of the panel with the number in parenthesis denoting the topoisomer on which the complex is based. (a) FCL minicircles. (b) L minicircles.

centred at −142 and −163, as well as the divergently transcribed *nifF* promoter. At high activator concentrations we would expect to detect the formation of open complexes at the *nifF* promoter in addition to those formed at *nifL* (Minchin et al., 1988). In contrast, the CL minicircle lacks the *nifF* promoter but retains the *nifL* promoter and the NTRC-binding sites. Both of the NTRC-binding sites are absent in the L minicircle. A fragment based on the *gln*Ap2 promoter was also constructed for comparative purposes. The *gln*Ap2 promoter contains five NTRC binding sites, of which the two distal sites are responsible for 85% of the transcriptional activity (Reitzer & Magasanik, 1986; Ninfa et al., 1987).

The electrophoretic properties of individual topoisomers of the FCL, L and C minicircles are shown in Figure 3. As expected, the presence of excess chloroquine which introduces positive writhe into each topoisomer, resulted in a successive decrease in electrophoretic mobility as the level of negative supercoiling increased (Figure 3a, lanes 1−12). In the absence of chloroquine, topoisomers differing by steps of a single linking number ($\Delta Lk = 1$) are expected to migrate with increasing velocity in acrylamide gels as the torsional stress increases. Thus in this gel system the FCL topoisomer denoted $\Delta Lk = 0$ had the slowest mobility, migrating close to the nicked species (Figure 3b, lane 2). The $\Delta Lk = +1$ and $\Delta Lk = -1$ topoisomers had similar mobilities whereas the $\Delta Lk = -2$ topoisomers showed the expected increases in electrophoretic mobility (compare Figure 3b, lanes 1 and 4). However the $\Delta Lk = -3$ topoisomer exhibited a

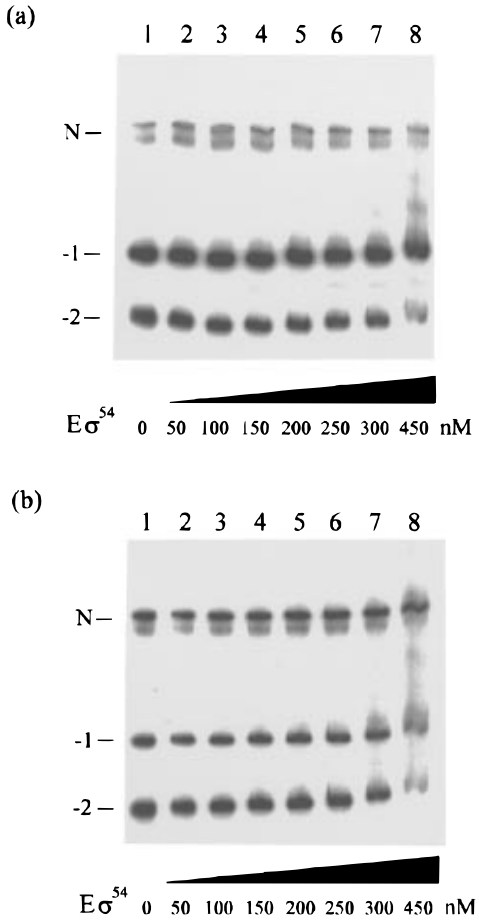

FIGURE 5: Binding of $E\sigma^{54}$ to mixed populations of −1 and −2 topoisomers carrying the *nifL* and *nifF* promoters. Reactions were performed in TAP buffer and complexes were allowed to form over 20 min at 37 °C in the presence of various concentrations of $E\sigma^{54}$ (expressed as the core RNA polymerase concentration with a 5-fold excess of σ^{54}) as indicated beneath each lane. Complexes were analyzed as described in the legend to Figure 4. (a) FCL minicircles. (b) FCL74 minicircles.

discontinuity in electrophoretic behavior since this species migrated close to the −1 topoisomer (Figure 3b, compare lanes 4 and 6). This aberrant electrophoretic mobility is indicative of a local structural transition perhaps, for example, reflecting Z DNA formation or cruciform extrusion. A similar discontinuity in electrophoretic behavior was found with the L minicircle (Figure 3b, lanes 7−9) suggesting that the apparent conformational change induced by negative supercoiling in not associated with either the upstream region of the *nifL* promoter or the *nifF* promoter. The CL minicircle apparently undergoes a similar structural transition between $\Delta Lk = -1$ and $\Delta Lk = -2$ (Figure 3b, lanes 10−12), consistent with the superhelical density of the −2 topoisomer of this minicircle (-0.06) being similar to that of the −3 topoisomer of the FCL minicircle ($\sigma = -0.066$).

Binding of NTRC and $E\sigma^{54}$ to Minicircles

The binding of phosphorylated NTRC to the FCL minicircle was investigated by gel retardation using three different topoisomers (Figure 4a). Although a bound complex was formed on each topoisomer at concentrations of NTRC−phosphate above 300 nM, smearing was visible at high protein concentrations (lanes 4, 8, and 12), indicative of protein dissociation during the gel run. Although the resolution of the shifted species is poor, it would appear that

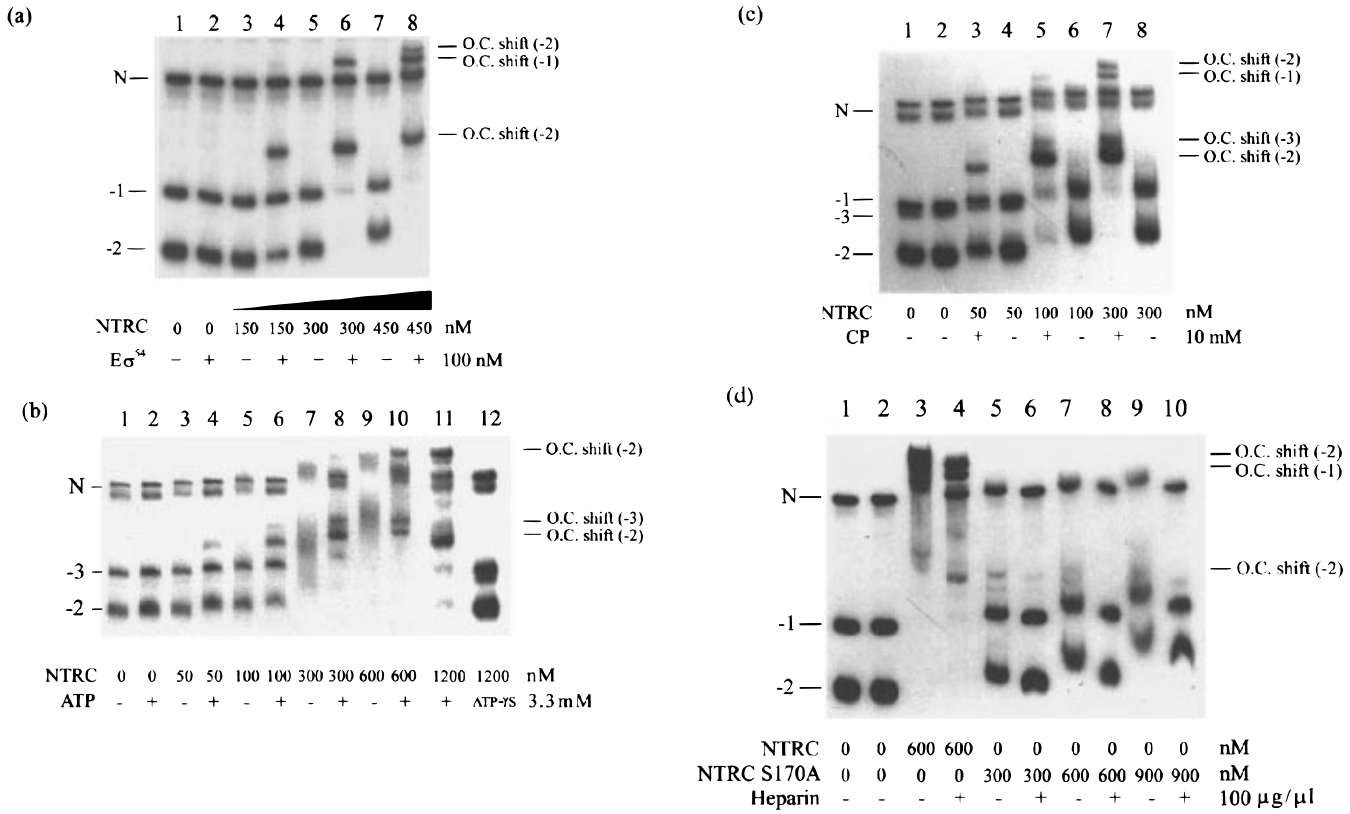

FIGURE 6: Requirements for the formation of open complex band shifts on mixed topoisomer populations. All reactions were incubated in TAP buffer for 20 min at 37 °C and, except where otherwise noted beneath each lane, contained core RNA polymerase (100 nM), σ^{54} (300 nM), carbamoyl phosphate (10 mM), ATP (3.3 mM), and sonicated salmon sperm DNA (3.4 mg L^{-1}). The NTRC concentration is also noted beneath each lane. Free topoisomers and protein−DNA complexes (denoted O.C.) are identified next to the relevant bands and the numbers in parentheses indicate the topoisomer upon which each shift is based. These assignments are based on the analysis of individual topoisomers (see Figure 7). Note that the −2 topoisomer gives two discrete band shifts. (a) Requirement for Eσ^{54}. (b) Requirement for ATP. Note that the reaction in lane 12 contained ATPγS in place of ATP. Heparin (final concentration 100 mg L^{-1}) was added to reactions in lanes 11 and 12 immediately prior to loading the gel. (c) Carbamoyl phosphate requirement. Note that lane 1 contained no Eσ^{54}. In addition to the components indicated, heparin (final concentration 100 mg L^{-1}) was added to reactions in lanes 11 and 12 immediately prior to loading the gel. (d) Influence of the mutant S170A form of NTRC. Where noted heparin (100 mg L^{-1}) was added to the reaction immediately prior to loading onto the gel. The reaction in lane 1 did not contain Eσ^{54}.

NTRC does not show a strong topoisomer preference, suggesting that it does not promote significant unwinding of DNA. A bound complex was not detectable at 300 nM NTRC on the L minicircle, (which lacks the NTRC sites) suggesting that the complex formed on the FCL template reflects site-specific DNA binding (Figure 4b).

In contrast we observed no binding of Eσ^{54} to a mixed population of −1 and −2 FCL topoisomers at concentrations up to 300 nM (expressed as core enzyme saturated with a 5-fold excess of σ^{54}) (Figure 5a). The smearing at high concentrations may reflect dissociation of weakly bound Eσ^{54} during the gel run or the formation of nonspecific protein−DNA interactions. Minicircles based on the mutant *nif*L74 promoter which has increased affinity for Eσ^{54} also produced no discrete shift (Figure 5b), even though binding of Eσ^{54} to this promoter can be detected in solution by dimethyl sulfate footprinting (Whitehall et al., 1992). This suggests that the interactions between the polymerase holoenzyme and the promoter are too weak to be visualized in this gel system. This observation is in accord with previous findings that σ^{54}-holoenzyme does not form a stable closed complex with the *nifL* promoter in the absence of NTRC (Minchin et al., 1989; Austin et al., 1991; Whitehall et al., 1992), and the current studies suggest that this may also be the case with the *nifF* promoter.

Formation of Open Promoter Complexes on Minicircles

When phosphorylated NTRC was incubated together with Eσ^{54} in the presence of ATP, the mobility of individual bands in mixed topoisomer populations decreased to a much greater extent than in the presence of NTRC alone (Figure 6a). These retarded species were assigned to shifts in the mobility of the −1, −2, and −3 topoisomers as determined by experiments with individual topoisomers (see below). Some complexes were formed at low activator concentrations when stable binding of NTRC alone was not observed (Figure 6, compare lanes 3 and 4 in each case). Formation of these discrete complexes required ATP (Figure 6b, lanes 1−10). At relatively high activator concentrations in the absence of ATP, smearing was visible, perhaps indicative of the formation of unstable closed complexes (Figure 6b, lanes 7 and 9). The formation of discrete complexes was not observed with the nonhydrolyzable analogue ATPγS indicating that ATP hydrolysis is required (Figure 6b, lanes 11 and 12). The accumulation of these complexes was also dependent on phosphorylation of NTRC (Figure 6c). Complexes formed at relatively high activator concentrations were stable to challenge by heparin (Figure 6b, lanes 10 and 11; Figure 6c, lane 7; Figure 6d, compare lanes 3 and 4), a characteristic feature of open promoter complexes.

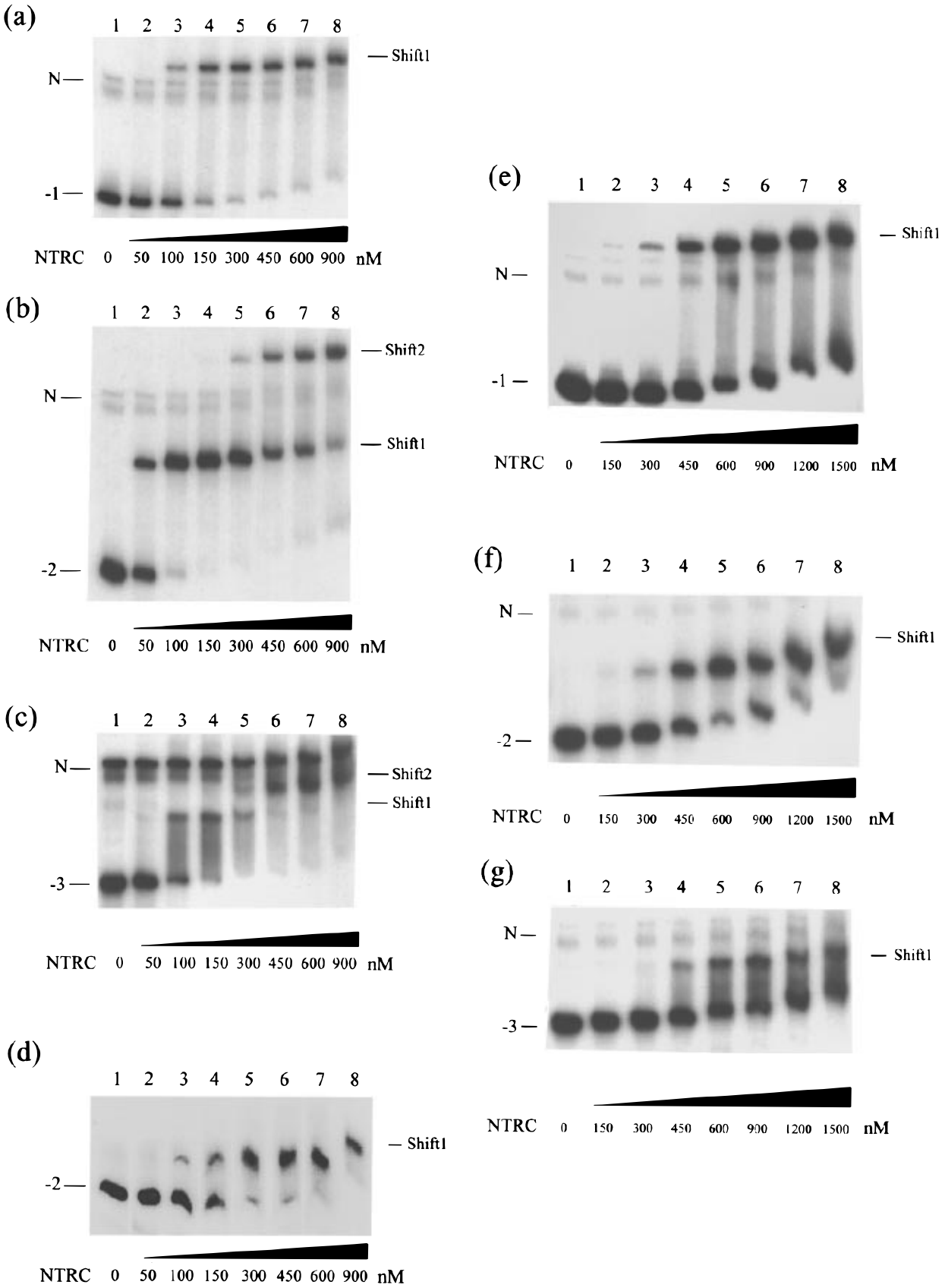

FIGURE 7: Influence of NTRC concentration upon open complex formation on individual topoisomers. Open complexes were formed on purified topoisomers as described in Experimental Procedures, using the NTRC concentrations indicated beneath each lane. (a) FCL −1 topoisomer, (b) FCL −2 topoisomer, (c) FCL −3 topoisomer, (d) CL −2 topoisomer, (e) L −1 topoisomer, (f) L −2 topoisomer, (g) L −3 topoisomer.

We have previously described the properties of the serine 170 to alanine (S170A) mutant form of NTRC which is competent to facilitate occupancy of the *nifL* promoter by $E\sigma^{54}$ but is defective in catalyzing the isomerisation of the closed complex to the open promoter complex (Austin et al., 1991). This protein did not give rise to the heparin-

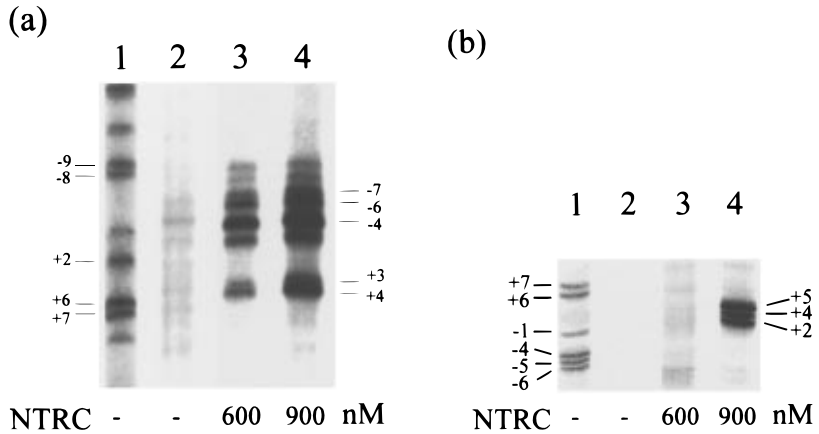

FIGURE 8: Probing open complexes formed at the *nifL* and *nifF* promoters on the FCL minicircle with potassium permanganate. Open complexes were allowed to form on a mixture of unlabeled −1 and −2 topoisomers of the FCL minicircle in the presence of the NTRC concentrations indicated beneath each lane and were then treated with $KMnO_4$; after digestion with *Bam*HI and *Alu*I they were 3′ end-labeled with Klenow polymerase and [α^{32}-P]dGTP to analyze the top strand as described in Experimental Procedures. Lane 1 in each case is a G-specific chemical cleavage reaction. (a) The *nifL* promoter analyzed on a "short" gel run. (b) *nifF* promoter analyzed on a "long" gel run.

resistant topoisomer shifts seen with wild-type NTRC (Figure 6d), also indicating that such shifts represent the formation of open promoter complexes.

Topoisomer Preference for Open Complex Formation on Negatively Supercoiled Templates

In order to assess the relative efficiency of open complex formation at different superhelical densities, individual topoisomers were incubated with Eσ^{54} and ATP in the presence of limiting concentrations of NTRC. Autoradiograms of a typical experiments with the FCL minicircle are shown in Figure 7. Each of the negatively supercoiled minicircles formed a discrete bound complex and in each case the mobility shift was indicative of unwinding of the topoisomer upon formation of the open promoter complex. For example in this electrophoresis system an unwinding of one helical turn would cause the −1 topoisomer to resemble the relaxed molecule but an additional shift is also expected due to protein binding. Thus the complex formed on the −1 topoisomer (shift 1) runs at a slower mobility than the relaxed minicircle (Figure 7a) and the complex on the −2 topoisomer runs above the free −1 topoisomer (Figure 7b). At relatively high NTRC concentrations, a second shift (shift 2) was detected on the −2 topoisomer which has a slower mobility than the relaxed molecule (Figure 7b, lanes 5−8). A second shift was also detected on the −3 topoisomer (Figure 7c). This shift could be due to further protein binding or DNA unwinding. However it was not detected when complexes were formed on −2 topoisomers of the CL minicircle which lacks the *nifF* promoter (Figure 7d), suggesting that it is representative of molecules in which open complexes have formed on both the *nifL* and *nifF* promoters. In accordance with this model the second shift was not observed on topoisomers of the L minicircle which lacks the *nifF* promoter as well as the NTRC binding sites (Figure 7e−g). Higher NTRC−P concentrations were required to form complexes on this template, consonant with the lack of specific binding sites on the L minicircle. However, the mobility of the shifted species on each L topoisomer was almost identical to that of shift 1 formed on the FCL minicircle. Hence the NTRC binding sites make little contribution to the mobility of the complexes although their presence facilitates complex formation at lower activator concentrations.

To further identify open complexes formed on the *nif*L and *nifF* promoters, mixed topoisomer populations ($\Delta Lk = -1, -2, -3$) of the FCL minicircle were subjected to potassium permanganate footprinting ($KMnO_4$) following incubation of reaction mixtures under the conditions used for the gel retardation assays. $KMnO_4$ preferentially oxidizes single-stranded T residues and can be used to probe for regions of DNA unwinding associated with open complexes (Sasse-Dwight & Gralla, 1988). At the *nifL* promoter, T residues on the top strand between −7 and +4 became hyper-reactive to $KMnO_4$ in the presence of Eσ^{54}, ATP, and NTRC−phosphate (Figure 8a). Reactivity was dependent on each of these additions indicative of the formation of open promoter complexes (data not shown). Similarly, T residues between +2 and +5 in the top strand of the *nifF* promoter became reactive to $KMnO_4$ (Figure 8b). However in this case a higher activator concentration was required, since reactivity was only strongly enhanced at 900 nM NTRC; in contrast the *nifL* promoter gave a notably stronger signal at 600 nM NTRC (compare lanes 3 and 4 in Figure 8a and 8b). Hyper-reactivity to $KMnO_4$ was not observed in the intergenic region between the two promoters (data not shown). These data taken together with the gel shift results strongly suggest that the topoisomer shifts defined as shift 1 and shift 2 are associated with open complex formation. The results also indicate that the *nifL* promoter opens at a lower NTRC concentration than that required for *nifF* and that isomerization of the *nifF* promoter is detected on minicircle molecules in which opening of the *nifL* promoter has already occurred.

At 300 nM NTRC−phosphate, complexes accumulated rapidly on the FCL template (within 1 min) and remained at a steady state level with no increase in accumulation over a 2 h period indicating that complex formation is limited by activator concentration. Complexes were stable to heparin challenge in solution for at least 60 min prior to loading the gel and the mobility of the heparin-challenged complexes was identical to those of the non-challenged species (data not shown). A series of titrations performed with the FCL template at varying activator concentrations indicated that

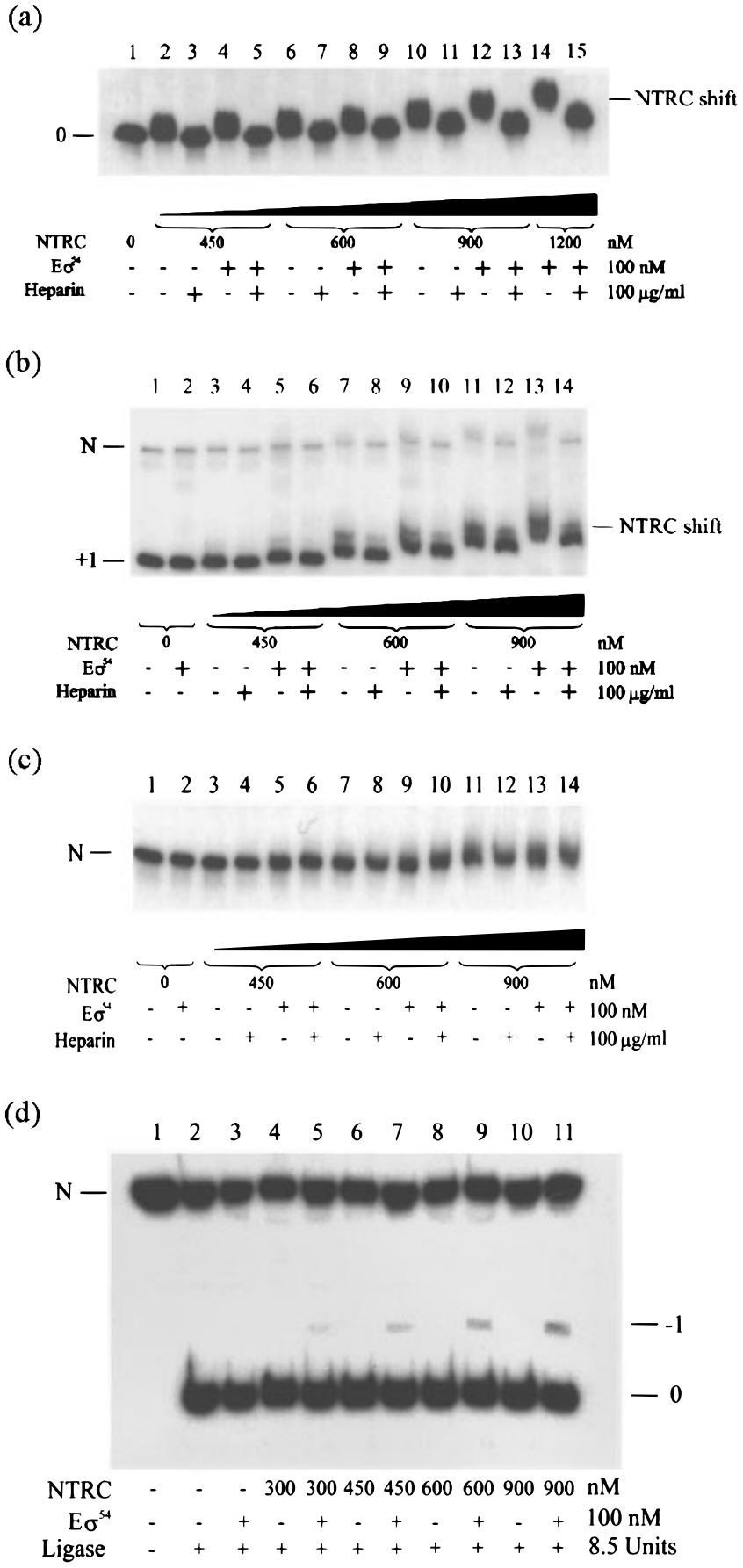

FIGURE 9: Analysis of complexes formed on minicircles with positive or zero linking difference. Complexes were formed under the conditions described in Experimental Procedures at various NTRC concentrations and the presence of Eσ^{54} as indicated beneath each lane. Where indicated heparin was added immediately prior to loading the gel. In panels a−c complexes of the FCL minicircle were analyzed by gel retardation analysis: (a) the relaxed topoisomer, (b) the +1 topoisomer, and (c) nicked circular DNA. In panel d, complexes preformed on the CL minicircle were treated with T4 DNA ligase and electrophoresed on a TBE gel containing chloroquine (7.5 mg L^{-1}).

the −1 topoisomer ($\sigma = -0.022$) is the least favored substrate and the −2 topoisomer ($\sigma = -0.044$) is slightly preferred over the -3 topoisomer ($\sigma = -0.066$). Thus the supercoiling response of the *nifL* promoter as measured on minicircles appears to be biphasic, as has been observed when this response is measured on larger plasmids (Whitehall et al., 1992).

Thermodynamic Constraints on Open Complex Formation: Comparison of the nifL and glnAp2 Promoters

We have previously proposed that the free energy of supercoiling is required to facilitate step(s) along the pathway of transcription initiation at the *nifL* promoter since linear DNA fragments and relaxed plasmid DNA are relatively poor templates for the formation of open promoter complexes. In contrast, open complex formation at the σ^{54}-dependent *glnA*p2 promoter is relatively insensitive to the level of DNA supercoiling. Since the torsional constraints imposed by DNA minicircles allow a more rigorous analysis of the thermodynamic requirements for open complex formation, we sought to determine whether open complexes at the *nifL* promoter would form on relaxed as well positively supercoiled minicircles. An unwinding of one helical turn on the relaxed minicircle would be expected to change the apparent linking number in the remainder of the molecule so that it resembles the +1 topoisomer. However, although NTRC−P alone bound to the relaxed FCL minicircle, we were unable to detect heparin resistant open complexes on the relaxed topoisomer (Figure 9a). Likewise we were unable to detect a shift representative of the open complex on the +1 topoisomer (Figure 9b).

The failure to observe formation of complexes on the relaxed and +1 species could reflect an inability to detect small changes in electrophoretic mobility or could result from the instability of such complexes in this particular gel system. We therefore examined whether open complexes would form on these topoisomers in solution by probing for the presence of locally melted DNA in the open complexes using $KMnO_4$ footprinting. As expected, promoter opening was observed on a mixture of the −2 and −1 topoisomers of the FCL minicircle with T residues at −5 to −2 on the bottom strand being hyper-reactive to $KMn0_4$ (Figure 10, lane 7). This reactivity was dependent on the presence of ATP in the incubation mixture consistent with the requirement for nucleoside triphosphate hydrolysis for open complex formation. In contrast, on the relaxed and +1 topoisomers there was no apparent enhancement of $KMnO_4$ reactivity in the −5 to −2 region (Figure 10, lanes 3 and 5) indicating that open complexes do not form on these topoisomers in solution.

To further confirm that DNA unwinding associated with open complex formation occurs on negatively supercoiled minicircles but not on the relaxed and +1 topoisomers, preformed nucleoprotein complexes formed on the CL minicircle were treated with topoisomerase I and the reaction products were analyzed on chloroquine gels. No unwinding was detected when only Eσ^{54} or NTRC−P was present (Figure 11, lanes 5−8) or when both proteins were incubated together in the absence of ATP (Figure 11, lanes 11 and 12). In conditions which favor open complex formation, topoisomerase treatment of negatively supercoiled minicircles produced the −1 topoisomer but no evidence for unwinding was observed on the relaxed minicircle or the +1 topoisomer (Figure 11, lanes 13 and 14). These results indicate that up to one helical turn of unwinding is constrained within open complexes formed on the negatively supercoiled topoisomers and in agreement with the gel retardation and $KMnO_4$ footprinting data, demonstrate that the formation of open promoter complexes on constrained DNA templates is dependent upon negative supercoiling.

The formation of open promoter complexes on relaxed and positively supercoiled minicircles requires an energetically unfavorable increase in writhe. No such topological change is necessary on linear or nicked DNA molecules since the strands are free to rotate around one another and any change in apparent ΔTw can be dissipated. No significant mobility change was detected when nicked minicircles were incubated with NTRC−P, Eσ^{54}, and ATP (Figure 9c) but open complexes formed on the nicked template would not be readily detected by gel retardation analysis if the majority of the shift seen with the constrained topoisomers is associated with DNA unwinding rather than protein binding. To determine if DNA unwinding associated with open complex formation occurs on nicked minicircles, preformed complexes were treated with DNA ligase and the products were analyzed on chloroquine gels (Figure 9d). As expected the major product of the ligation reaction was the $\Delta Lk = 0$ topoisomer and no evidence for DNA unwinding was observed with either NTRC−P or Eσ^{54} alone. Under the conditions required for open complex formation the −1 topoisomer was also a ligation product indicating that open complex formation can occur on nicked minicircles. Similar results were obtained when linear DNA was used as template (data not shown).

We were interested to determine whether the topoisomer selectivity observed with the *nifL* promoter also applied to the σ^{54}-dependent *glnA*p2 promoter which is relatively insensitive to changes in DNA supercoiling (Whitehall et al., 1992). Unfortunately we were unable to resolve topoisomers of *glnA*p2 minicircles in the Tris-glycine gel system so studies of these minicircles were confined to the analysis of open complexes in solution. Complexes formed on purified topoisomers were probed by $KMnO_4$ footprinting. In contrast to the *nifL* promoter, we observed $KMnO_4$ hyperreactivity between −9 and +3 on the bottom strand, indicative of open complex formation on the relaxed DNA and the +1 topoisomer, as well as on the negatively supercoiled topoisomers (Figure 10, lanes 3, 5, and 7). To demonstrate that this hyper-reactivity does indeed represent unwinding in the open complex on these *glnA*p2 topoisomers, preformed complexes were subjected to topoisomerase treatment and analyzed on chloroquine gels (Figure 12). Surprisingly, when NTRC−phosphate was incubated with minicircles, the +1 topoisomer was generated in addition to relaxed DNA after topoisomerase action and removal of the bound protein (Figure 12, lanes 8, 11, and 14). It seems highly unlikely that NTRC can constrain a region of increased twist and since we do not observe similar results with *nifL* minicircles (Figure 11) or with larger plasmids containing the *glnA*p2 promoter (unpublished data), we believe this may be an experimental artifact in which the topoisomer equilibrium is displaced.

When all the components necessary for open complex formation were present, i.e., NTRC, Eσ^{54}, and ATP, the −1 topoisomer was detected, irrespective of the superhelical

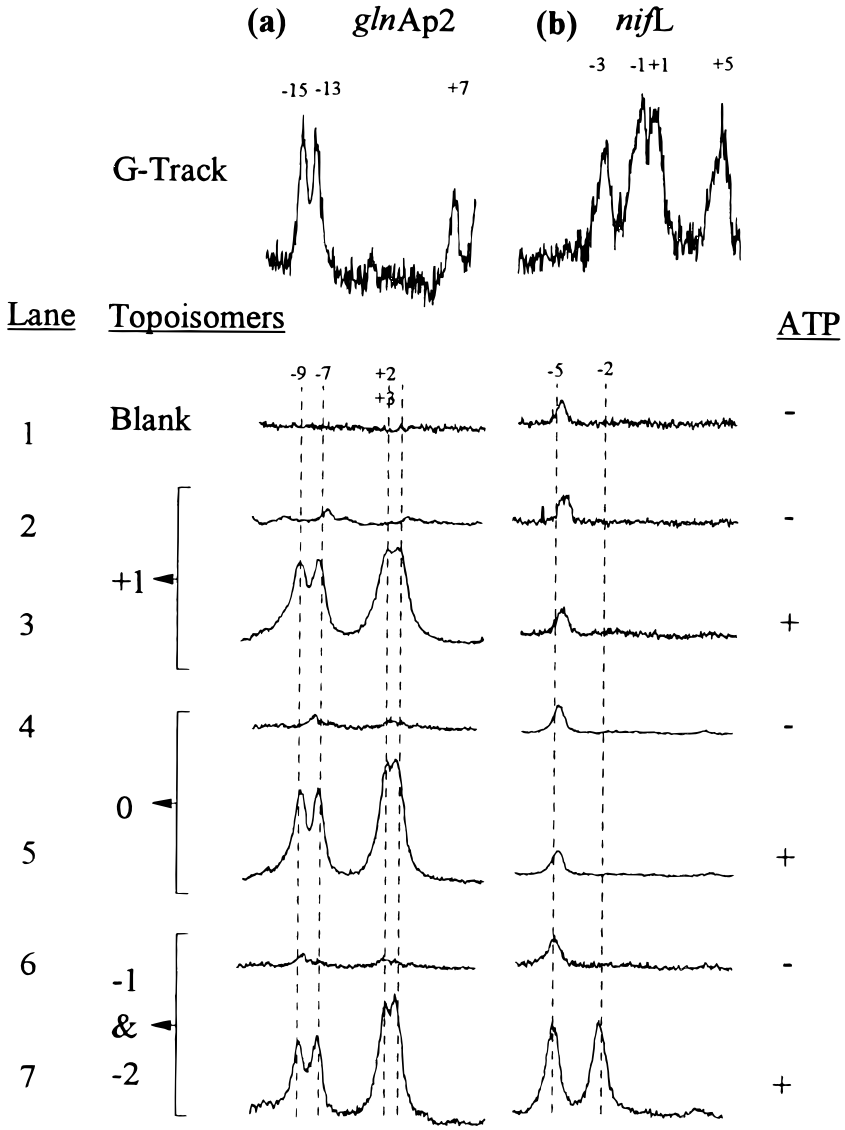

FIGURE 10: Comparative potassium permanganate footprints of open promoter complexes formed on discrete topoisomers carrying either the *glnA*p2 or *nifL* promoters. Complexes were formed under the conditions described in Experimental Procedures using prelabeled minicircles to allow analysis of the bottom strand. The products were electrophoresed on 6% polyacrylamide sequencing gels and then scanned using a Molecular Dynamics computing densitometer. Column a indicates scans of the CG minicircle (*glnA*p2 promoter) on reactions containing 300 nM NTRC, and column b shows the FCL minicircle (*nifL* promoter) at 900 nM NTRC. The top row shows scans of G-specific chemical cleavage reactions on an untreated mixture of the −1 and −2 topoisomers. Lane 1 is derived from $KMnO_4$ reactions with a mixture of the −1 and −2 topoisomers in which Eσ^{54} and ATP were omitted. ATP was also omitted from reactions in lanes 2, 4, and 6. Topoisomers analyzed by $KMnO_4$ footprinting were +1 (lanes 2 and 3), relaxed (lanes 4 and 5), and a mixture of −1 and −2 (lanes 6 and 7).

density of the minicircle on which the complexes were preformed (Figure 12, lanes 7, 10, 13, and 16). This indicates that up to one helical turn of unwinding is constrained following topoisomerase action, confirming that open complexes are formed on the relaxed template. The data do not unequivocally demonstrate that complexes are formed on the +1 topoisomer (Figure 12c) since complexes could be formed after the topoisomerase action. Nevertheless the data in Figure 10 strongly suggest that complex formation occurs on the +1 topoisomer since there was little contaminating nicked or relaxed DNA in purified preparations of this topoisomer (Figure 12c, lane1). Thus the pathway of open complex formation at the *glnA*p2 promoter is independent of the free energy of DNA supercoiling and unwinding occurs even on relaxed or positively supercoiled topoisomers where it is energetically unfavorable.

DISCUSSION

DNA minicircles have a number of advantages over the use of larger plasmids for studying the supercoiling response of promoters since the properties of individual topoisomers can be examined rather than averaging results from a mixed population of topoisomers with a range of linking differences. In this study the minicircle assay has proven useful not only for analyzing topological requirements for the formation of open complexes but also as an indication of the structural properties of the promoters. Comparison of the mobilities of topoisomers of the *nifL* minicircles suggest that a structural transition occurs at superhelical densities of −0.06 or lower. The precise location and nature of the transition is unknown, although since it occurs on the FCL, CL, and L templates it must be localised downstream of the NTRC binding sites. One possibility is that a region rich in alternating (C-G)

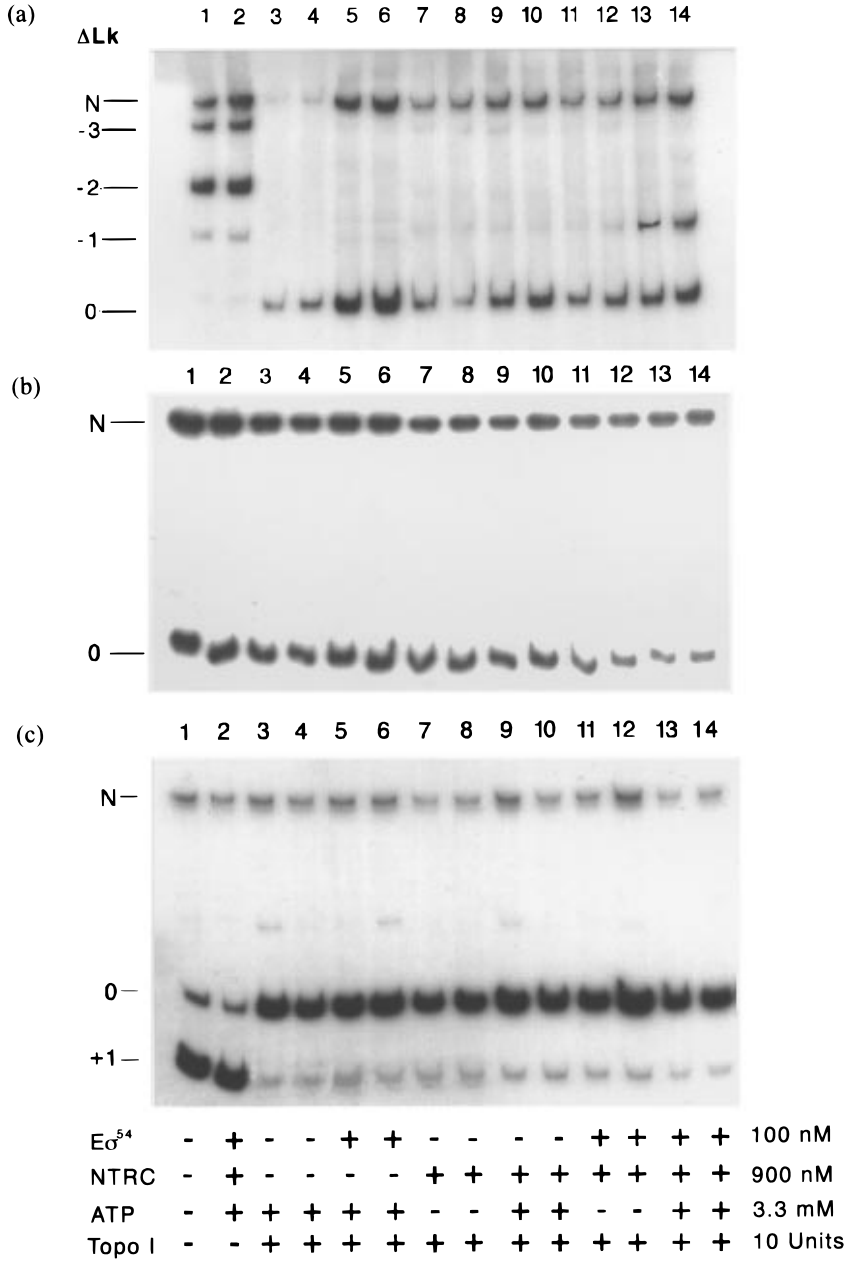

FIGURE 11: Topoisomerase treatment of complexes formed on CL minicircle topoisomers. Complexes were formed in TAP buffer under the conditions described in Experimental Procedures with the components indicated beneath each lane. Complexes were then treated with topoisomerase I and electrophoresed on TBE gels containing chloroquine (7.5 mg L^{-1}). Lanes 3−14 show reactions carried out in duplicate. (a) −2 and −3 topoisomers. (b) Relaxed topoisomer. (c) +1 topoisomer.

which falls between the NTRC binding sites and the Eσ^{54} recognition sequences (Drummond et al., 1983) undergoes a B-Z DNA transition. The ability of such sequences to form Z DNA in minicircle topoisomers and on plasmids and chromosomes has been well documented (Nordheim & Meese, 1988; Zacharias et al., 1988; Rachmouni & Wells, 1989; Rachmouni, 1992; Gruskin & Rich, 1993).

We observe quantitative formation of open promoter complexes on minicircles indicating that small constrained DNA molecules provide useful models for transcriptional activation studies. Since no significant band shifts were detectable on nicked circular DNA it is probable that a large component of the mobility shift upon open complex formation is due to changes in the topology of the minicircle. The contribution of DNA loop formation, between upstream bound activator and promoter-bound Eσ^{54}, to this shift appears to be negligible as the mobilities of complexes formed on the FCL and L minicircles are identical. Assuming that the majority of the shift represents the topological change associated with DNA unwinding, then a melted region of approximately 10 base pairs is expected in the open complex at *nifL*, consistent with the appearance of the −1 topoisomer after topoisomerase I treatment of preformed complexes and the extent of the $KMn0_4$ footprint. The mobility change associated with the second complex (shift 2) resulted in the −2 topoisomer running above nicked circular or relaxed minicircles, which is consistent with an additional unwinding of approximately one helical turn at the *nifF* promoter. Quantitative analysis of topoisomer shifts on minicircles carrying the σ^{70}-dependent TAC promoters suggests an unwinding of approximately 0.9 turns associated with the open complex (Su & McClure, 1994).

Minicircles impose topological restictions upon DNA unwinding and can be considered as models for constrained

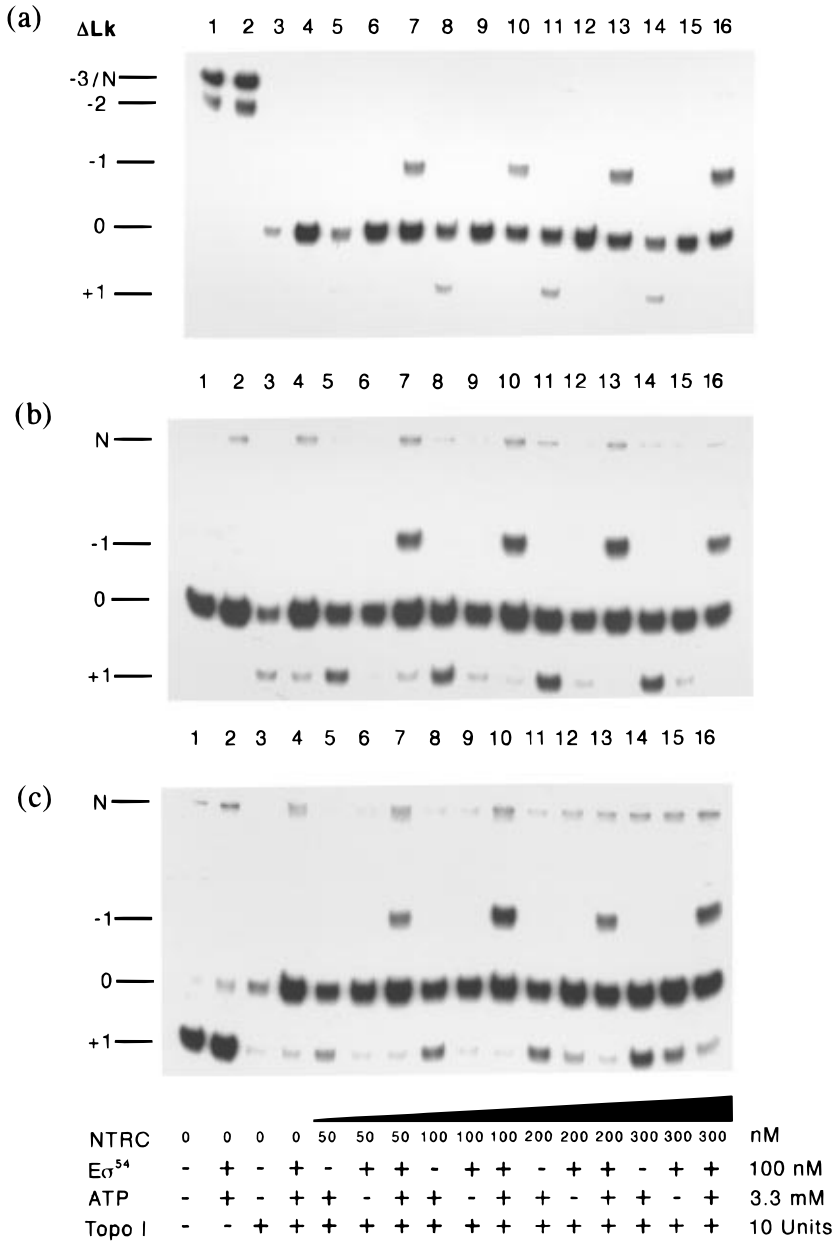

FIGURE 12: Topoisomerase treatment of complexes formed on CG minicircle topoisomers. Complexes were formed and analyzed as in Figure 11. (a) −2 and −3 topoisomers, (b) relaxed topoisomer (c) +1 topoisomer.

superhelical domains. Biophysical experiments with small DNA circles suggest that the free energy of supercoiling increases with decreasing DNA length so that writhing of the helix axis is disfavored as the circle size decreases (Shore & Baldwin, 1983; Horowitz & Wang 1984). However physiological concentrations of counterions allow small circles to adopt a tighly interwound conformation allowing significant partitioning of the linking number deficit as writhe (Bednar et al., 1994). We anticipated that the open complexes would not be formed on relaxed or positively supercoiled minicircles since their formation would not be thermodynamically favored. In a closed molecule, strand separation will lead to a change in ΔTw which must be compensated by an equivalent change in ΔWr because the ΔLk of a closed molecule cannot be altered without strand breakage. The formation of open complexes on negatively supercoiled molecules is energetically favorable since it leads to a decrease in ΔWr, making the topoisomer adopt a conformation closer to that of relaxed DNA. In contrast, promoter melting on relaxed or positively supercoiled minicircles would lead to an increase in writhe and hence requires an energy input. Hence although the *nifL* promoter can support open complex formation on topologically nonconstrained templates such as linear and nicked circular DNA, it cannot do so on relaxed closed circular DNA or the $\Delta Lk = +1$ topoisomer. A comparable energetic barrier has been observed with minicircles carrying the σ^{70}-dependent *lac*UV5 promoter. Whereas open promoter complexes are readily formed on negatively supercoiled minicircles, the $\Delta Lk = 0$ topoisomer favors the formation of the closed, rather than the open promoter complex (Kahn & Crothers, 1993). Energetic considerations may also explain why the second mobility shift (shift 2), which represents open complex formation at both the *nifF* and *nifL* promoters, was detected on the −2 and −3 topoisomers but not on the −1 topoisomer. Assuming that strand separation leads to an unwinding of around one helical turn at both of these promoters, the free energy of DNA supercoiling could be

utilized to form the first complex on the −1 topoisomer but an equivalent input of energy would be needed to form the second open complex on this topoisomer (Figure 13).

In contrast to the situation with the *nifL* promoter, there appears to be little topological barrier to the formation of open promoter complexes by σ^{54}-holenzyme at the *glnAp*2 promoter since open complexes were formed on all the topoisomers examined including the +1 topoisomer. In this case the contribution of ATP hydrolysis by the activator to strand separation by the polymerase may therefore overcome the thermodynamic barrier imposed by the torsional constraint. Formation of open complexes at the *glnA*p2 promoter therefore requires less free energy than at the *nifL* of *nifF* promoters and as a consequence the activation of these *nif* promoters is more sensitive to the level of negative DNA supercoiling.

Many, but not all σ^{54}-dependent promoters contain sites for the integration host factor (IHF) located between the enhancer binding sites and the RNA polymerase recognition sequence (Pérez-Martín et al., 1994). IHF stimulates open complex formation at such promoters by bending the intervening DNA to facilitate interaction between upstream bound activator and downstream bound polymerase. Neither the *glnA*p2 nor the *nifL* promoters contain IHF binding sites and the torsional flexibility of the intervening DNA may play an important role in determining productive interactions between activator and polymerase at these promoters. In the case of *glnA*p2 the intervening DNA is presumed to be intrinsically curved (Carmona & Magasanik, 1996) while at the *nifL* promoter the bending energy associated with long-distance interactions could be offset by the free energy of DNA supercoiling (Whitehall et al., 1993). Although the bending free energy may impose thermodynamic constraints on DNA strand separation, this is unlikely to be the sole factor which distinguishes the *glnA*p2 from the *nifL* promoters, particularly since the experiments reported here were performed at "high" activator concentrations which allow activation in the absence of the enhancer binding sites.

One of the most important factors in determining the thermodynamic requirements for open complex formation at these promoters is likely to be the nature of the sequence in the melted region. This sequence is more G·C rich in the *nifL* and *nifF* promoters than *glnA*p2. Mutations in the *nifL* promoter at −3 and −1 which increase the A·T content of this sequence alter the supercoiling response so that the promoter is more active at low superhelical densities. In addition these mutations increase the stability of open complexes formed on linear DNA (Whitehall et al., 1992). Conversely, mutations in the melted region of the *glnA*p2 promoter which increase its G·C content, significantly decrease the half-life of open complexes on linear DNA and open complexes formed on this variant *glnA*p2 promoter decay back to the closed complex, indicating that there is a thermodynamic barrier to open complex formation by σ^{54}-holoenzyme under these conditions (Wedel & Kustu, 1995). We therefore propose that the sequence of the melted region is a major factor in determining thermodynamic requirements for open complex formation at σ^{54}-dependent promoters. At the *nifL* and *nifF* promoters the standard free energy of the open complex is probably greater than that of the closed complex, and negative supercoiling can provide an energetic contribution. In contrast, at the *glnA*p2 promoter the net free energy change upon open complex formation must be sufficiently negative to accommodate an increase in writhe in the constrained minicircle (Figure 13).

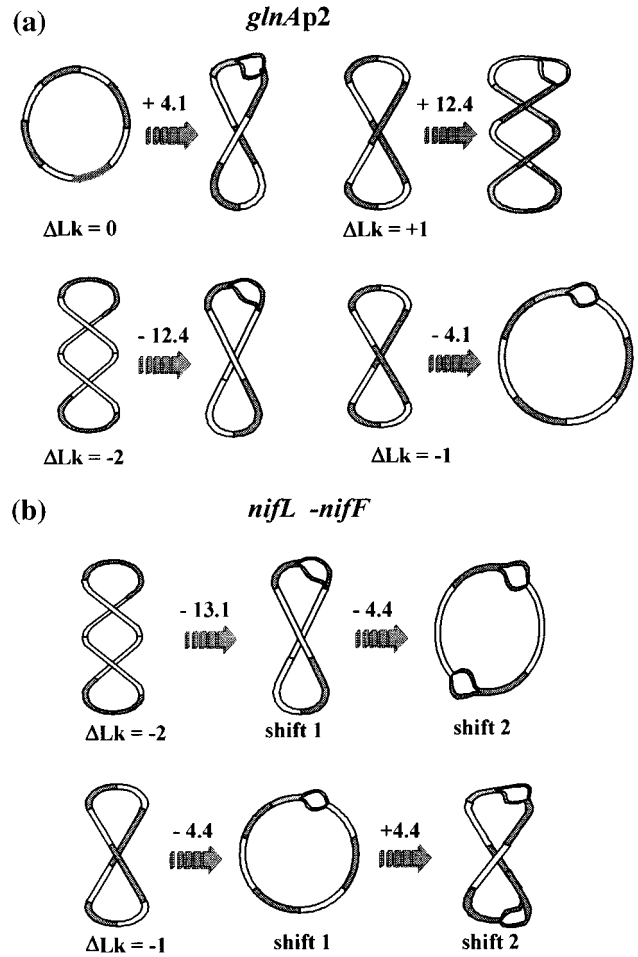

FIGURE 13: Topological consequences of open complex formation on individual topoisomers and thermodynamic implications. In all cases it is assumed that open complex formation by σ^{54}-RNA polymerase introduces approximately one helical turn of unwinding at each promoter (see Figures 11 and 12). The values above the arrows are the predicted supercoiling free energy changes ($\Delta\Delta G$) in kcal/mol using the data of Horowitz and Wang (1984) and extrapolating NK for the 475 bp *nifL* and 498 bp *glnA*p2 minicircles from the plot of NK verses N. These values are likely to be considerably smaller if writhing in small circles is more favorable in the presence of counter ions (Bednar et al., 1994). (a) Substrates for open complex formation at the *glnA*p2 promoter. DNA strand separation on the relaxed (ΔLk = 0) and the +1 topoisomers introduces a turn of positive writhe, requiring an input of free energy. We propose that the overall free energy change upon open complex formation at this promoter is sufficiently negative to accommodate the increase in writhe. In contrast, negatively supercoiled topoisomers are favorable substrates for open complex formation since unwinding decreases the torsional stress within the molecule. (b) Topological consequences of open complex formation on the FCL minicircle which contains both the *nifL* and *nifF* promoters. Since the relaxed and +1 topoisomers cannot be utilized as substrates for open complex formation on this minicircle we propose that there is a greater thermodynamic constraint upon the formation of open complexes at *nifL* compared with *glnA*p2 and that the supercoiling free energy of the negatively supercoiled topoisomers is utilized to favor DNA strand separation. As shown here open complex formation on the −2 topoisomer (ΔLk = −2) gives rise to either a single open complex (shift 1) or to open complex formation at both the *nifL* and *nifF* promoters (shift 2). The predicted decrease in writhe in both of these cases is thermodynamically favorable. In contrast, and in accordance with our observations, only a single shift is favored on the −1 topoisomer (ΔLk = −1) since the formation of a second complex is predicted to lead to an increase in writhe.

Studies with mutant forms of σ^{54} which, to a certain extent bypass the requirement for NTRC, suggest a two-step model for transcriptional activation in which the activator initially induces melting of the promoter by the holenzyme to form an unstable open complex which is further converted by the activator to a more stable heparin resistant form (Wang & Gralla, 1997). It has been proposed that these steps ensure that transcription initiation by the σ^{54} holoenzyme is completely activator dependent. The sequence of the melted region could impose a further check upon the DNA unwinding function of the holoenzyme at certain promoters by increasing the thermodynamic barrier to the formation of the initial open complex, effectively restricting the process of activation to nucleoprotein complexes in which negative torsional stress facilitates the unwinding reaction. This torsional strain could also be utilized to stabilize the open complex in the proposed second step of the mechanism since we find that open complex formation is relatively inefficient on linear DNA templates and the complexes formed on linear DNA are less extensive and more unstable than those formed on supercoiled DNA (Whitehall et al., 1992).

Nitrogen fixation is an energy intensive process requiring at least 16 mol of ATP per mole of dinitrogen fixed (Eady, 1995). The *nifL* promoter provides a major checkpoint for controlling transcription of the *nif* regulon ensuring that nitrogenase is only expressed under nitrogen-limiting conditions when NTRC is phosphorylated. The negative supercoiling dependence of the transcriptional activation pathway at this promoter provides an additional thermodynamic checkpoint on gene expression, which is probably modulated by the ATP/ADP ratio *in vivo* since the level of negative DNA supercoiling is dependent on phosphorylation potential (van Workum et al., 1996). In contrast, the *glnA*p2 promoter controls expression of a key enzyme required for ammonium assimilation under nitrogen limiting conditions. In common with all σ^{54}-dependent promoters, open complex formation at *glnA*p2 is kinetically coupled to ATP hydrolysis by the activator (Wedel & Kustu, 1995) and in this case an input of negative torsional stress is unnecessary since the structure of the promoter allows DNA melting on linear templates even in the absence of DNA chaperones such as IHF (Carmona & Magasanik, 1996).

ACKNOWLEDGMENT

We thank Martin Buck, Mark Buttner, and Gary Sawers for their critical comments on the manuscript.

REFERENCES

Austin, S., Kundrot, C., & Dixon, R. (1991) *Nucleic Acids Res. 19*, 2281−2287.
Bates, D., & Maxwell, A. (1989) *EMBO J. 8*, 1861−1866.
Bednar, J., Furrer, P., Stasiak, A. Dubuchet, J., Egelman, E. H., & Bates, D (1994) *J. Mol. Biol. 235*, 825−847.
Buck, M., Cannon, W., & Woodcock, J. (1987) *Mol. Microbiol. 1*, 243−249.
Carmona, M., & Magasanik, B. (1996) *J. Mol. Biol. 261*, 348−356.
Dimri, G. P., & Das, H. K. (1988) *Mol. Gen. Genet. 212*, 360−363.
Dixon, R. (1984) *Nucleic Acids Res. 12*, 7811−7830.
Dixon, R., Henderson, N. C., & Austin, S. (1988) *Nucleic Acids Res. 16*, 9933−9946.
Dorman, C. J., Barr, G. C., NiBriain, N., & Higgins, C. F. (1988) *J. Bacteriol. 170*, 2816−2826.
Douc-Rasy, S., Kolb, A., & Prunell, A. (1989) *Nucleic Acids Res. 17*, 5173−5189.
Drummond, M., Clements, J., Merrick, M., & Dixon, R. (1983) *Nature 301*, 302−307.
Eady, R. R. (1995) *Sci. Prog. 78*, 1−17.
Elliot, T., & Geiduschek, E. P. (1984) *Cell 36*, 211−219.
Gruskin, E. A., & Rich, A. (1993) *Biochemistry 32*, 2167−2176.
Horowitz, D. S., & Wang, J. C. (1984) *J. Mol. Biol. 173*, 75−91
Hseih, L. S., Burger, R. M., & Drlica, K. (1991) *J. Mol. Biol 219*, 443−450.
Kahn, J. D., & Crothers, D. M. (1993) *Cold Spring Harbor Symp. Quant. Biol. 58*, 115−122.
Kramer, H., Amouyal, M., Nordheim, A., & Muller-Hill, B. (1988) *EMBO J. 7*, 547−566.
Kranz, R. G., & Haselkorn, R. (1986) *Proc. Natl. Acad. Sci. U.S.A. 83*, 6805−6809.
Kustu, S., Santero, E., Keener, J., Popham, D., & Weiss, D. (1989) *Microbiol. Rev.* 53, 367−376.
Lavigne, M., Kolb, A., Yeramian, E., & Buc, H. (1994) *EMBO J.* 13, 4983−4990.
Merrick, M. J. (1993) *Mol. Microbiol. 10*, 903−909
Minchin, S. D., Austin, S., & Dixon, R. A. (1988) *Mol. Microbiol. 2*, 433−442.
Minchin, S. D., Austin, S., & Dixon, R. A. (1989) *EMBO J. 8*, 3491−3499.
Ninfa, A. J., Reitzer, L. J., & Magasanik, B. (1987) *Cell 50*, 1039−1046.
Nordheim, A., & Meese, K. (1988) *Nucleic Acids Res. 16*, 21−37.
Pérez-Martín, J., Rojo, F., & de Lorenzo, V. (1994) *Microbiol. Rev. 58*, 268−290.
Rachmouni, A. R. (1992) *Mol. Microbiol 6*, 569−572.
Rachmouni, A. R., & Wells, R. D. (1989) *Science 246*, 358−363.
Reitzer, L. J., & Magasanik, B. (1986) *Cell 45*, 785−792.
Reitzer, L. J., Movsas, B., & Magasanik, B. (1989) *J. Bacteriol. 171*, 5512−5522.
Sasse-Dwight, S., & Gralla, J. D. (1988) *Proc. Natl. Acad. Sci. U.S.A. 85*, 8934−8938.
Shore, D., & Baldwin, R. L. (1983) *J. Mol. Biol. 170*, 957−981.
Su, T. T., & McClure, W. R. (1994) *J. Biol. Chem. 269*, 13511−13521.
Su, W., Porter, S., Kustu, S., & Echols, H. (1990) *Proc. Natl. Acad. Sci. U.S.A. 87*, 5504−5508.
van Workum, M., van Dooren, S. J. M., Oldenburg, N., Molenaar, D., Jensen, P. R., Snoep, J. L., & Westerhoff, H. V. (1996) *Mol. Microbiol. 20*, 351−360.
Wang, J. T., & Gralla, J. D. (1997) *J. Biol. Chem. 271*, 32707−32713.
Wedel, A., & Kustu, S. (1995) *Genes Dev. 9*, 2042−2052.
Wedel, A., Weiss, D. S., Popham, D., Droge, P., & Kustu, S. (1991) *Science 248*, 486−490.
Whitehall, S., Austin, S., & Dixon, R. (1992) *J. Mol .Biol. 225*, 591−607.
Whitehall, S., Austin, S., & Dixon, R. (1993) *Mol. Microbiol. 9*, 1107−1117.
Zacharias, W., Jaworski, A., Larson, J. E., & Wells, R. D. (1988) *Proc. Natl. Acad. Sci. 85*, 7069−7073.

BI9701179